

MODELING OF EX-VESSEL MELT POOL COOLABILITY UNDER BOTTOM FLOODING WITH DECAY HEAT SIMULATION

Nitendra SINGH^{1,2}, Parimal P. KULKARNI¹ and Arun K. NAYAK*¹

¹: Reactor Engineering Division, Bhabha Atomic Research Centre, Mumbai 400085, Maharashtra, India

²: Faculty of Engineering Sciences, Homi Bhabha National Institute, Anushakti Nagar, Mumbai 400094, Maharashtra, India

nitendrasingh1988@gmail.com; parimalk@barc.gov.in; arunths@barc.gov.in

ABSTRACT

Nuclear accident at Fukushima has brought a significant change towards severe accident research for advancement in nuclear safety. The societal and political impact of radioactivity leakage into the environment has demanded further robustness in the line of defense of nuclear safety. Thus, the coolability and stabilization of corium within the reactor containment in case of severe accident scenario is still a challenging issue. In order to ensure this, many new reactors have been envisaged with core catcher. In a core catcher, melt pool coolability is one of the biggest concerns. In spite of several efforts, melt pool coolability is poorly understood phenomenon so far. After studying the various cooling strategies, it has been demonstrated that melt coolability using bottom flooding is one of the most efficient techniques so far.

A model has been developed for the study of melt pool coolability under bottom flooding with decay heat simulation. This model postulates the formation of crust below the melt pool when water is being flooded from the bottom. This crust is then subjected to various stresses leading to the failure of this crust resulting in the inverted conical melt eruption. The model captures this 'eruption cone' along with radial variation in porosity in it. The boiling heat transfer considered between the melt and the water results in a rapid and significant heat transfer during the melt quenching.

The model predictions have been compared with the experimental measurements. The results show that the model is able to capture the multidimensional temperature fields in the melt pool during the cooling process quite accurately.

KEYWORDS

Melt coolability, Bottom Flooding, Decay heat, Core catcher, Severe accidents

1. INTRODUCTION

Nuclear severe accident scenario is a concern for the nuclear reactors designers to provide the safest possible reactors compared to other energy sources. Nuclear industry has witnessed three major severe accidents with radioactivity release and core melt scenarios including Fukushima. To address consequences of such accidents, severe accident management (SAM) strategy is now practiced. The stabilization and termination of core meltdown scenario are the key points in SAM strategy. This core melt or corium can be quenched and cooled either in-vessel or outside the vessel using an

¹ Corresponding author

arrangement called as ex-vessel core catcher. The concern is to achieve rapid quenching and complete cooling of corium inside the core catcher.

Among the various cooling strategies adopted so far to quench and cool the melt, flooding the melt from top is the most eventual one. This is a simplest approach to execute, however, it may not be able to cool the entire melt due to the formation of thick crust and water ingress was limited to a few millimetres (Nayak et al., 2005; Sehgal et al., 2006; Nayak et al., 2009; Kulkarni et al., 2011). Kulkarni and Nayak (2014) studied different approaches for quenching and cooling of the melt have demonstrated that it took several hours to cool the melt with top flooding and side cooling even without decay. They also clearly concluded that the bottom flooding approach is the most effective technique for quenching and cooling the melt.

In bottom flooding approach, the water is introduced directly into the melt from bottom using nozzles which results in the formation of porous debris and enhances the coolability significantly. Experimental and numerical studies have been performed at various laboratories. COMET experimental series at FZK and ANL (Tromm et al., 1993; Alsmeyer and Tromm, 1995; Tromm and Alsmeyer, 1995; Alsmeyer et al., 1998; Foit et al., 2008) demonstrated the concept of melt coolability using bottom flooding approach. DECOBI experimental program at Royal Institute of Technology took further the issue of ex-vessel melt coolability using the bottom flooding approach and developed a model to understand the melt coolability phenomena observed in COMET experimental series (Paladino et al., 1999a, 1999b and 2002). A strenuous effort was instilled by Paladino et al. (2002) and Widmann et al. (2006) for the modelling of melt coolability with a focus to predict the porosity after the bottom coolant injection and its effect on coolability. Using the MEWA code, Foit et al. (2008) studied the quenching behaviour of different melt layers and the porosity formation. Kulkarni and Nayak (2013) presented a simple yet effective model for the fracture of crust formed under bottom flooding scenario while accounting for the thermal stresses acting on the crust.

Even though the model presented by Kulkarni and Nayak (2013) helps in understanding the basic philosophy melt pool coolability under bottom flooding but has some limitations in modelling of eruption cone, porosity variation in porous zone, decay heat simulation and boiling heat transfer between the melt and the water. Thus, this paper presents numerical modelling of melt coolability with decay heat under bottom flooding. This model extends the previous model which postulated the formation of crust below the melt pool when water is being inserted from the bottom. This crust is then subjected to various stresses leading to the failure of this crust resulting in the inverted cone shaped melt eruption. The model captures this 'eruption cone' along with radial variation in porosity. The boiling heat transfer considered between the melt and the water resulted in good prediction of melt pool temperatures. This model was used to predict the melt pool temperatures and the predictions were compared with the measurements obtained from the experiment by Singh et al (2015). Both the results are found to be in good concurrence with each other. These results show that quenching behaviour of the melt pool can be done within a few minutes.

2. EXPERIMENT

The melt coolability under bottom flooding with decay heat simulation, experiment referred throughout in this paper for the validation of the model, was conducted by Singh et al. (2015). The test section used for carrying out these experiments consisted of two parts viz. lower part for melt retention from furnace, water inlet and melt quenching, and upper part for steam expansion and its outlet. The temperatures inside the melt pool were measured by K-type thermo-couples arranged spatially at three radial and nine axial locations. To simulate the decay heat, 10 radiative heaters were used to directly heat the melt pool from outside. About 25 litres of borosilicate glass melt at initial temperature of nearly 1200°C was used as melt simulant. The melt was poured into the test section from the cold crucible induction furnace to form the melt pool in the lower part of the test section. Then, water was injected into the melt pool by using six nozzles located at the bottom of the melt

pool. The entire melt was quenched and cooled within a few minutes after the insertion of water. The measurements from this experiment have been used to compare and validate the model presented in this paper.

3. MODEL

The model presented in this paper is an extension of the simple model deduced by Kulkarni and Nayak (2013) to understand bottom flooding. The modifications and postulations of this model are done based on experimental data. The salient features of this model are given below.

3.1. Postulations

The basic postulates of this model are as follows, and depicted pictorially in figure 1.

- 1) When water is flooded into the melt through nozzles it interacts with water and cools down while forming a thin crust (Fig 1(a)).
- 2) This crust starts growing further upon addition of water (Fig 1(b)).
- 3) Due to heat transfer, steam forms and expands below the crust and exerts pressure on it.
- 4) The crust is now subjected to stresses
 - a) Steam pressure on one side
 - b) Hydrostatic head of the melt pool on the other side
 - c) Thermal stresses generated due to temperature gradient across the thickness
- 5) When the total stresses exceed fracture stress, the melt erupts forming an inverted cone shaped porous zone called as 'eruption cone' (Fig 1(c) and 1(d)).
- 6) This eruption cone acts as the passage for cooling fluids and has a radially varying porosity.
- 7) Boling heat transfer occurs between the melt and the cooling fluids in this eruption cone which is quite significant and rapid.
- 8) These result in enhancement of melt coolability significantly.

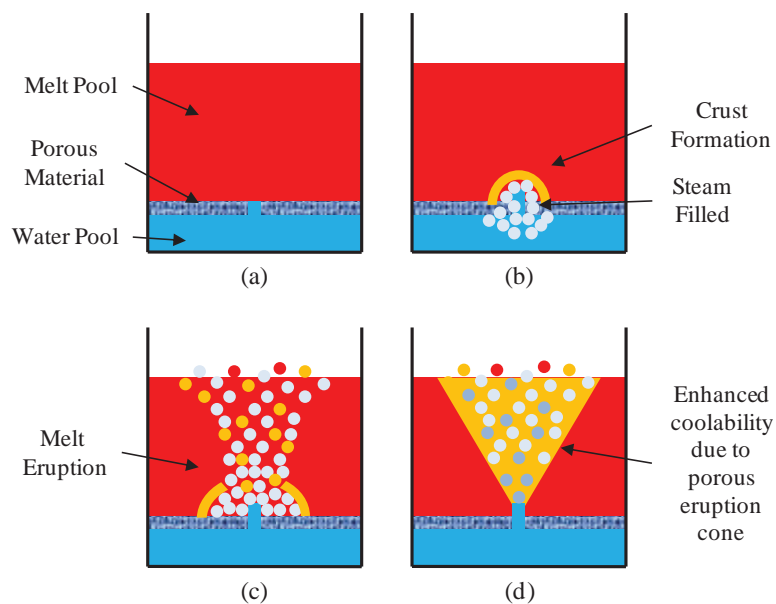


Figure 1: Melt coolability under bottom flooding with decay heat model

3.2. Limitations of Existing Model

3.2.1. Eruption cone versus cylindrical porous channels

In the model by Kulkarni and Nayak (2013), it was assumed that the melt eruption forms the vertical porous channels with uniform porosity throughout this eruption zone, as shown in figure 2. One of the important limitations was the unaccountability heat sink. The heat transfer from porous debris, of the previous model, to coolant was considered to be by convection only and no phase change was involved. This boiling heat transfer is substantial.

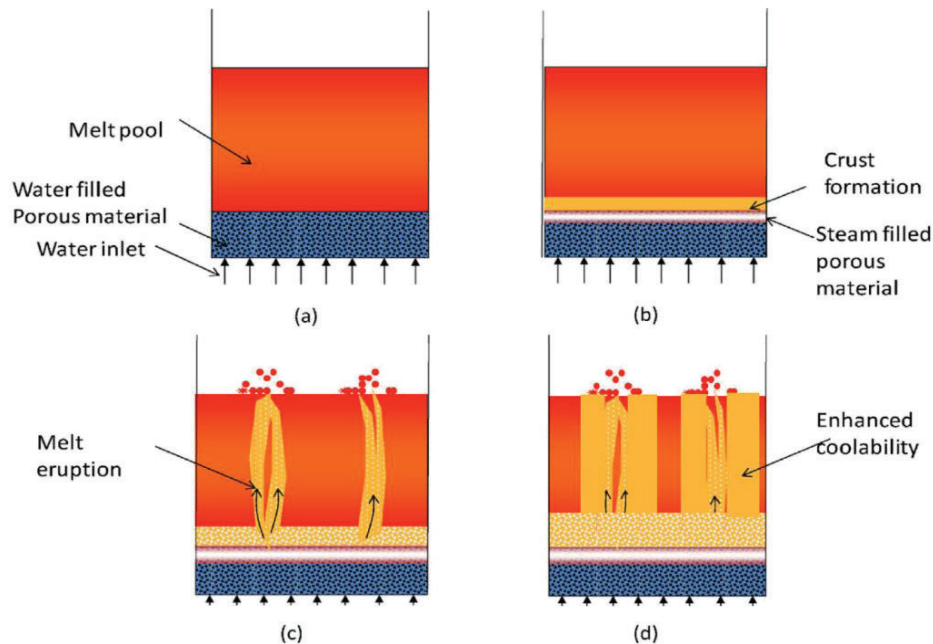


Figure 2: Melt coolability model by Kulkarni and Nayak (2013)

3.2.2. Porosity variation

In the experiments by Singh et al (2015), porous eruption cone was observed instead of vertical porous channels. It has also been observed that the porosity follows the radial variation in the eruption zone. Measurements of porosity show that the variation was radially decreasing within the eruption zone, as shown in figure 3. Due to this variation in porosity, the melt coolability also varies along the radius of the eruption zone.

3.3. Governing Equations

3.3.1. Governing equations for molten pool

Once the melt pool is formed in the ex-vessel severe accident scenario, conduction is the dominating mode of heat transfer. The transient two dimensional axi-symmetric heat conduction equation for the melt pool can be written as the following,

$$\rho C_p \frac{\partial T}{\partial t} = \frac{1}{r} \frac{\partial}{\partial r} r \left(k \frac{\partial T}{\partial r} \right) + k \frac{\partial^2 T}{\partial z^2} + q''' \quad \dots(1)$$

In the crust layer also, similar heat conduction equation is obeyed,

$$\rho C_p \frac{\partial T}{\partial t} = \frac{1}{r} \frac{\partial}{\partial r} \left(r k \frac{\partial T}{\partial r} \right) + k \frac{\partial^2 T}{\partial z^2} + q''' \quad \dots(2)$$

The boundary conditions for the above equations are given in Figure 4.

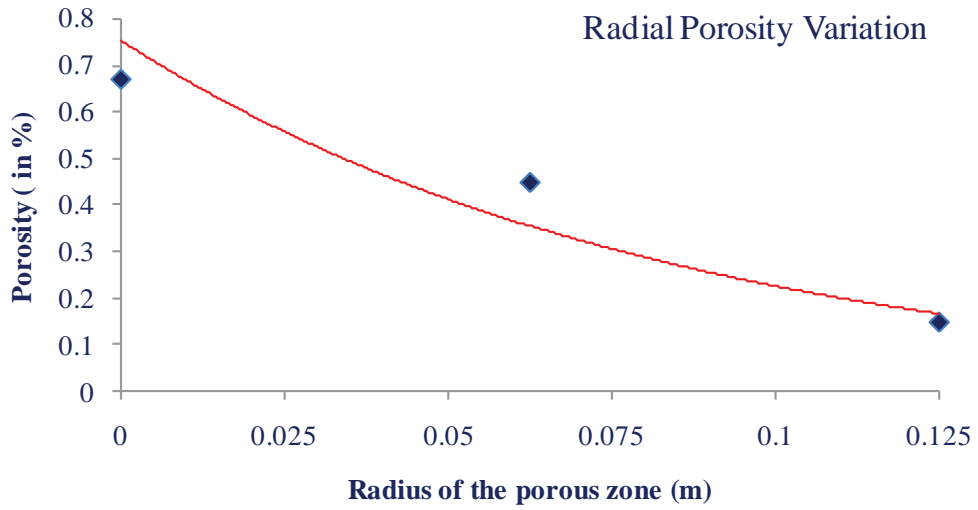


Figure 3: Variation in porosity along the radius of the porous zone within the test section

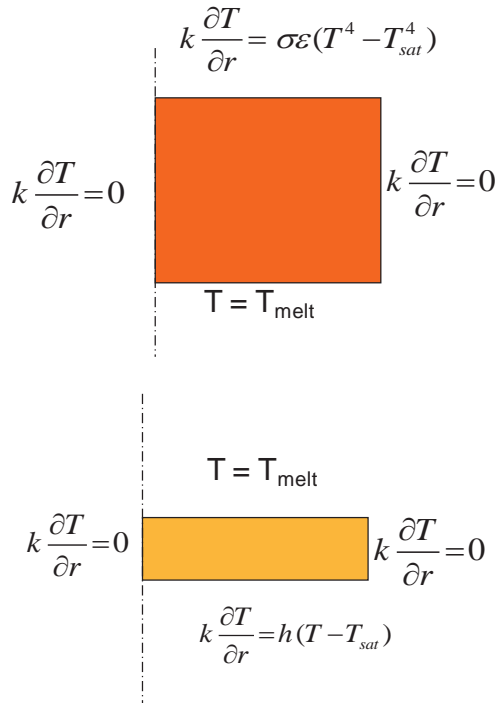


Figure 4: Boundary conditions for melt and crust layer.

3.3.2. Stresses in the crust

The crust is subjected to stresses as shown in Figure 5. The melt pool exerts hydrostatic head on the top of the crust while at the bottom of it, steam pressurizes it. In addition to this, the top edge of the crust is at melting temperature whereas; the bottom end is at much lower water temperature. This exerts thermal as well as mechanical stresses to the crust.

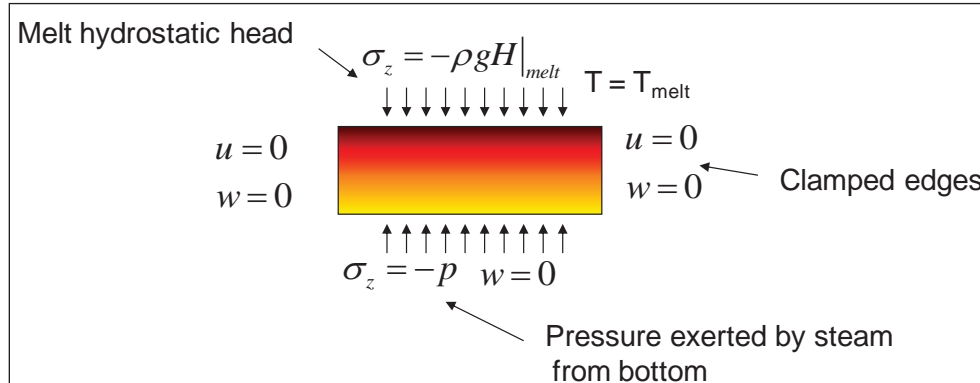


Figure 5: Stresses in the crust.

The bending stresses on the circular plate type crust as a result of clamped edges are given as (Timoshenko, 1959)

$$\sigma_b = 0.75 \cdot \frac{(\Delta p \cdot r^2)}{t_{cr}^2} \quad \dots (3)$$

The thermal stresses as a result of temperature gradient are given as

$$\sigma_{th} = \frac{\alpha \cdot \Delta T \cdot E}{2(1-\nu)} \quad \dots (4)$$

Since the total strain is additive and the material, being brittle, remains in elastic region, hence, we can add the individual stresses to obtain the total maximum stress acting on the crust as

$$\sigma_{tot} = \sigma_{th} + \sigma_b \quad \dots (5)$$

The crust will break if the total stress exceeds the strength of the crust i.e.

$$\sigma_{tot} > \sigma_{max} \quad \dots (6)$$

After the crust is broken, melt eruption starts to occur at nozzle locations. The eruption cone contains many channels through which mixture of steam and water flows. The location of these channels within the eruption cone is random in nature. However we can estimate the distribution of these channels within the eruption cone. Paladino et al (2002)

has developed an empirical model for density of the openings and their diameter. Using this, the average number of channels is given as

$$\Psi = \frac{\Gamma [Cp_w \cdot \Delta T_{sub} + h_{fg} + Cp_{st} \cdot \Delta T_{sup}]_c}{h_{pool} \cdot A_{ch} \cdot N_n \cdot \overline{\Delta T_{m,w}}} \quad \dots (7)$$

Where, $\overline{\Delta T_{m,w}}$ is average temperature drop between melt and water.

The average density of channels per unit area can be given as

$$\gamma = \frac{1}{\xi^2} \quad \dots (8)$$

Where ξ is the spacing between the channels given by Zuber's (1958) modified Critical Taylor Wavelength formula as

$$\xi = 2\pi \sqrt{\frac{\sigma_{mc}}{(\rho_m - \rho_{st})g}} \quad \dots (9)$$

The diameter of the channel is given as

$$d = 2 \sqrt{\frac{\Psi}{\gamma\pi}} \quad \dots (10)$$

Once the crust is broken, the melt layer is considered to be made of two zones, mainly porous zone and non-porous zone.

3.3.3. Equation in porous zone

Energy balance equation for the porous zone can be written as below

$$\rho C_P \frac{\partial T}{\partial t} = \frac{1}{r} \frac{\partial}{\partial r} r \left(k \frac{\partial T}{\partial r} \right) + k \frac{\partial^2 T}{\partial z^2} + q''' - q_{s,f}''' \quad \dots (11)$$

This equation includes the decay heat term, q''' , and the heat sink term, $q_{s,f}'''$, considering that a unit volume of porous medium completely transfers the heat to the cooling fluid passing through it.

The interfacial area density is obtained from porosity and the particle diameter, d_p is,

$$\dot{a} = 6 \frac{(1 - \varepsilon)}{d_p} \quad \dots (12)$$

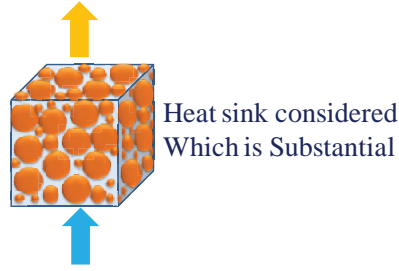


Figure 6: Philosophy of the present model

The heat transfer from solid to fluid acts as a heat sink term,

$$q'''_{s,f} = h \cdot \dot{a} \cdot (T - T_{inf}) \quad \dots (13)$$

Where, h is evaluated from surface temperature based on heat transfer regime i.e. film boiling or nucleate boiling. In the model, for film boiling, Berenson's (1963) model is used and for nucleate boiling, Rohsenow (1952) correlation is used.

As observed in the experiments, porosity varies as a function of radius of the porous zone, $\varepsilon = \mathcal{F}(r)$. The correlation for the radial porosity variation has been deduced from the test data and is given by

$$\varepsilon = 0.753 e^{-11.9 r} \quad \dots (14)$$

The model predicts the temperatures in the melt pool by modifying the initial domain and governing equations by using effective properties as

$$\rho_{eff} = \rho_{fluid} \cdot \varepsilon + \rho_{solid} \cdot (1 - \varepsilon) \quad \dots (15)$$

The equation for porous medium is modified as

$$\rho_{eff} \cdot C_{p,eff} \cdot \frac{\partial T}{\partial t} = \frac{1}{r} \frac{\partial}{\partial r} r \left(K_{eff} \frac{\partial T}{\partial r} \right) + K_{eff} \cdot \frac{\partial^2 T}{\partial z^2} + q''' - h \cdot 6 \frac{(1 - \varepsilon)}{d_p} \cdot (T - T_{inf}) \quad \dots (16)$$

The effective properties are volume averaged over the void fraction in bed.

With boundary conditions as

$$k_{eff} \frac{\partial T}{\partial z} = h(T - T_{\infty}) \quad \dots (17)$$

For the solid zone, the boundary conditions are modified as shown in Figure 7. In addition to top and bottom, now the span of the solid zone has reduced and additional convective boundary condition at one side has been introduced which makes it coolable from two dimensions. As a result, the overall coolability is greatly enhanced.

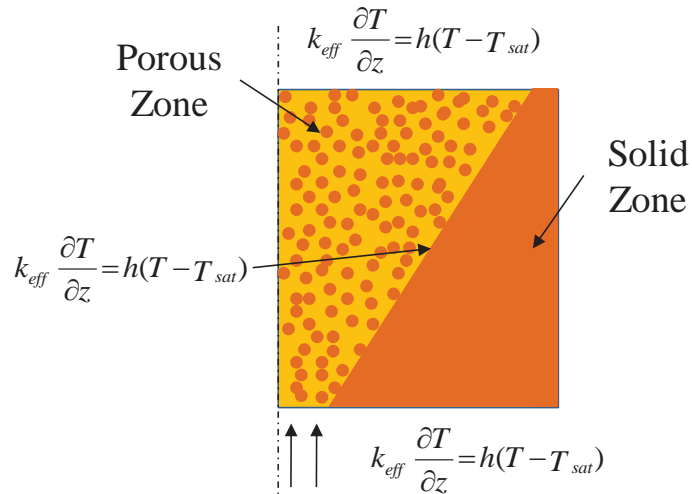


Figure 7: Modified boundary conditions for the domain

3.4. Solution Procedure

Finite difference method has been used for discretizing governing equations in the melt pool and solid crust region. Melt pool temperatures are obtained by implicitly solving these discretized equations using iterative Gauss-Seidel method. Once temperatures are evaluated, growth of the crust is calculated and subsequently the thickness of the solid crust region is updated. After the temperature distribution has been obtained, the stresses are calculated. With the stresses, the fracture conditions are evaluated. When the crust breaks, it is considered to be a porous zone with experimentally observed porosity and calculated number of eruption sites and diameter of eruption sites are calculated. After that, the domain is modified and the equations for porous zone and solid zones are recalculated using modified governing equations using similar technique.

4. RESULTS AND DISCUSSION

The predictions by the presented model were compared with the experimental measurements by Singh et al (2015).

The variation in melt pool temperatures at the central region is shown Figure 8. Both, numerical prediction and experimental measurements are following the trend and are in good agreement with each other.

Melt pool temperatures variation at half radius region is shown in figure 9. This is the region of highest porosity and implies to be the eruption site both numerically and experimentally. Due to the highest porosity in this region, there is sharp fall of temperatures. After the sharp fall in the experimental temperature, there is a rise in temperature due to the steady state water inlet flow rate which equals to the rate of steam formation. This has been modeled by changing the boundary condition as sink temperature, i.e. $T_{inf} = T_{sat}$ (water saturation temperature). Hence, there is a jump in temperature. The plot shows a good agreement in prediction and experimental measurements.

Figure 10 shows the variation in melt pool temperatures near wall region. The porosity was found to be the least in this region and hence the fall of temperatures was slower than other regions. The model predictions in this region too are following the experimental trend.

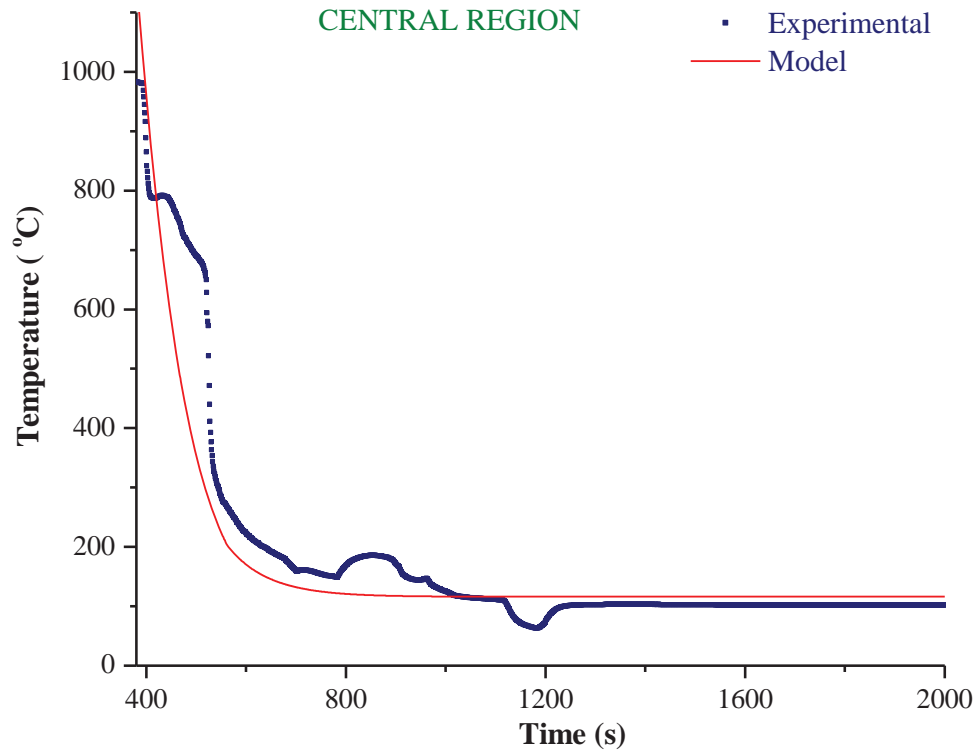


Figure 8: Modeled vis-à-vis measured temperatures at central location of the test section

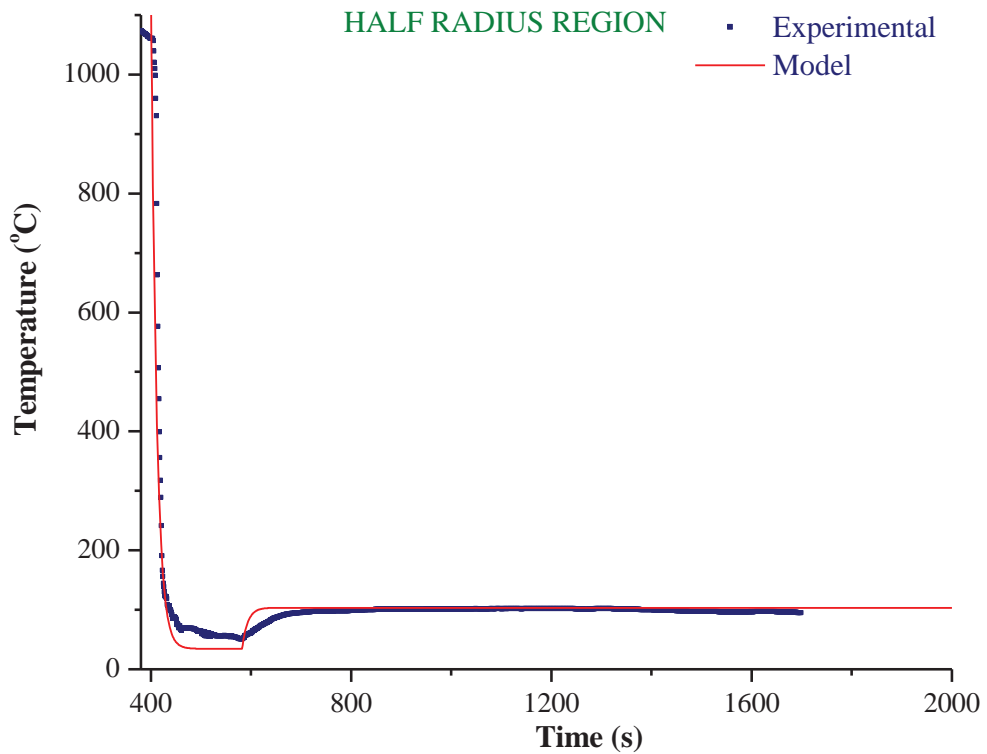


Figure 9: Modeled vis-à-vis measured temperatures at Half Radius of the test section

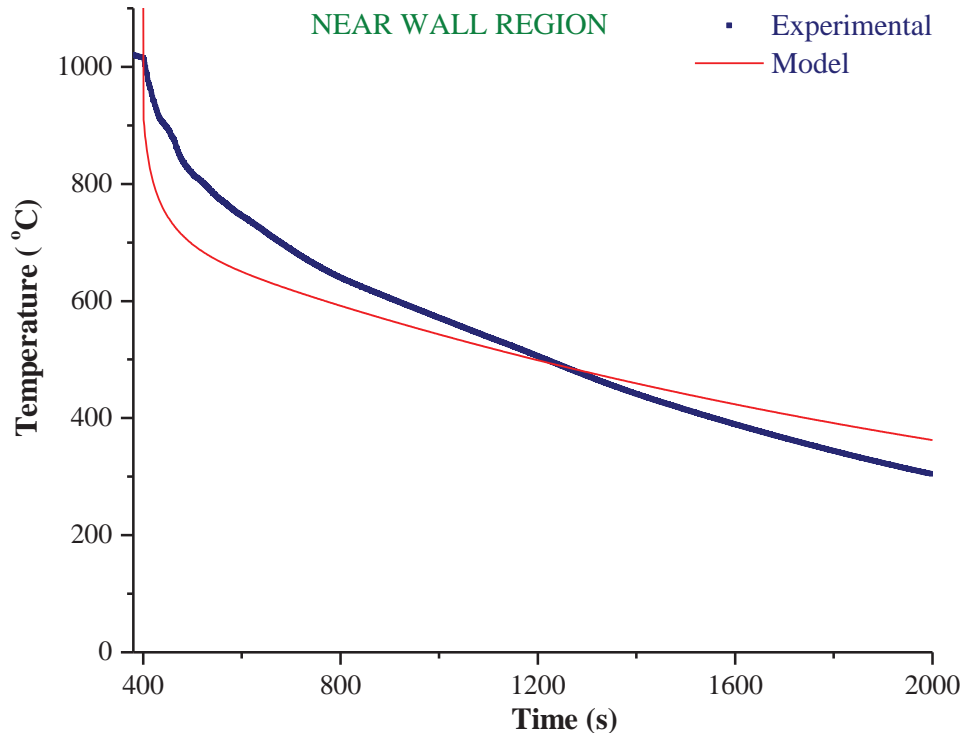


Figure 10: Modeled vis-à-vis measured temperatures near inner wall of the test section

5. CONCLUSIONS

Quenching and coolability of the molten corium during severe accident scenarios is one of the biggest challenges. For better understanding of melt pool coolability under bottom flooding with decay heat simulation, experiment has been conducted and a numerical model has been developed. The key inferences obtained from these measurements and predictions are as follows:

- The variation in porosity follows the below mentioned empirical relation within the eruption zone.

$$\varepsilon = 0.753 e^{-11.9 r}$$

- The heat transfer between melt and the cooling fluid is through boiling. Accounting the heat sink term in the energy balance equation predicts better estimates of melt pool temperature variations.
- It has been observed both numerically and experimentally, that the quenching of the melt takes place within a few seconds and the cooling of the debris also achieved within a few minutes under bottom flooding even in the presence of decay heat.

It can thus be concluded that presented model is able to capture the melt pool temperature variations during the coolability under bottom flooding with decay heat simulation. This model can be used for the estimation of actual reactor scenarios and the duration of melt pool cooling can be well predicted. The paper also emphasizes that the bottom flooding technique to quench and cool the melt pool is far efficient from any other approach for the ex-vessel scenario.

NOMENCLATURE

d	diameter (m)
g	Gravitational acceleration (m/s^2)
h	Heat transfer coefficient ($W/m^2 K$)
h_{bed}	Bed height (m)
h_{fg}	Latent heat of vaporization (J/kg)
h_{in}	Inlet enthalpy (J/kg)
h_{fs}	Liquid saturation enthalpy (J/kg)
k	Thermal Conductivity ($W/m K$)
p	Pressure (Pa)
q'''	Volumetric heat generation rate (W/m^3)
r	Radial direction (m)
t	Time (s)
t_{cr}	Crust thickness (m)
v	Velocity (m/s)
z	Axial direction (m)
A	Cross section area (m^2)
A_{ch}	Area of openings
C_p	Specific heat capacity at constant pressure (J/kg K)
D_n	Diameter of nozzle
E	Young's modulus (N/m^2)
L_b	Length of the opening
M	Mass (kg)
N_n	Number of inlet nozzles
T	Temperature (K)
V	Volume (m^3)
V_p	Volume in porous region

Greek letters

α	Linear expansion coefficient (K^{-1})
ε	Bed porosity
γ	Density of openings per unit area
κ	Bed permeability
μ	Viscosity (Pa.s)
ν	Poisson's ratio
ρ	Density (kg/m^3)
σ_b	Bending stress (N/m^2)
σ_{max}	Fracture stress (N/m^2)
σ_{mc}	Surface tension between melt and steam
σ_{th}	Thermal stress (N/m^2)
ξ	Critical Taylor wavelength
ψ	Number of eruption channels
Γ	Vapour generation rate (kg/s)

Subscripts

c	Crust
in	Inlet
l	Liquid
f	Fluid
m	Melt
nb	Nucleate boiling
r	Radial
s	Solid
st	Steam
sat	Saturation
sub	Subcooled
sup	Superheated
w	Water
v	Vapor
z	Axial

REFERENCES

1. A. K. Nayak, B. R. Sehgal, R. S. Rao, "Study on water ingression phenomenon in melt coolability," *Proceedings of International Topical Meeting on Nuclear Reactor Thermal-Hydraulics (NURETH-11)* pp. 449, Avignon, France, (2005).
2. B. R. Sehgal, "Stabilization and termination of severe accidents in LWRs," *Nucl. Eng. Des.* **236**, pp. 1941–1952 (2006).
3. A. K. Nayak, R. K. Singh, P. P Kulkarni, B. R. Sehgal, "A numerical and experimental study of water ingression phenomena in melt pool coolability," *Nucl. Eng. Des.* **239**, pp. 1285–1293 (2009).
4. P. P Kulkarni, R. K. Singh, A. K. Nayak, P. K. Vijayan, D. Saha, R. K. Sinha, "Physics of coolability of top flooded molten corium," *Proceedings of International Topical Meeting on Nuclear Reactor Thermal Hydraulics (NURETH-14)*, Toronto, Ontario, Canada, September 25–30, 2011, pp. 328 (2011).
5. P. P Kulkarni, A. K. Nayak, "Study on coolability of melt pool with different strategies," *Nucl. Eng. Des.* **270**, pp. 379–388 (2014).
6. W. Tromm, H. Alsmeyer, H. Schneider, "Fragmentation of melts by water inlet from below," *Proceedings of International Topical Meeting on Nuclear Reactor Thermal-Hydraulics (NURETH-6)* Grenoble, France, (1993).
7. H. Alsmeyer, W. Tromm, "Concept of a core cooling system and experiments performed," *Nucl. Eng. Des.* **154**, pp. 69–72 (1995).
8. W. Tromm, H. Alsmeyer, "Experiments for a core concept based on water addition from below," *Nucl. Eng. Des.* **157**, pp. 437– 445 (1995).
9. H. Alsmeyer, M. Farmer, F. Ferderer, B. Spencer, W. Tromm, "The COMET concept for cooling of ex-vessel corium melts," *Proceedings of International conference on Nuclear Engineering(ICONE-6)*, San Diego, CA, May10–14, 1998, pp. 6086 (1998).
10. J. J. Foit, M. Bürger, C. Journeau, H. Alsmeyer, W. Tromm, "Quenching of melt layers by bottom injection of water in the COMET core-catcher concept," *European Review Meeting Severe Accident Res., (ERMSAR)*, Nessebar, Bulgaria, 23–25 September, 2008 (2008).
11. D. Paladino, A. Theerthan, B. R. Sehgal, "Experimental Investigation on Debris Coolability by Bottom Injection," *ANS, Annual Meeting*, Boston, USA. (1999).
12. D. Paladino, A. Theerthan, L. Yang, B. R. Sehgal, "Experimental Investigations on Melt-Coolant Interaction Characteristics During Debris Cooling by Bottom Injection," *OECD Workshop on Ex-vessel Debris Coolability*, Karlsruhe, Germany (1999).
13. D. Paladino, A. Theerthan, B. R. Sehgal, "DECOBI: Investigation of Melt Coolability with Bottom Coolant Injection," *Prog. Nucl. Energy* **40**, pp. 161–206 (2002).

14. W. Widmann, M. Bürger, G. Lohnert, H. Alsmeyer, W. Tromm, “Experimental and theoretical investigations on the COMET concept for ex-vessel core melt retention,” *Nucl. Eng. Des.* **236**, pp. 2304–2327 (2006).
15. P. P Kulkarni, A. K. Nayak, “A simple model to understand physics of melt coolability under bottom flooding,” *Nucl. Eng. Des.* **262**, pp. 81–87 (2013).
16. Nitendra Singh, P. P. Kulkarni, A. K. Nayak, “Experimental investigation on melt coolability under bottom flooding with and without decay heat simulation,” *Nucl. Eng. Des.* **285**, pp. 48–57 (2015).